

## **PHASE DIAGRAM CALCULATIONS FOR THE ZnSe – BESE SYSTEM BY FIRST-PRINCIPLES BASED THERMODYNAMIC MONTE CARLO INTEGRATION**

**ANDRZEJ WOŹNIAKOWSKI, JÓZEF DENISZCZYK\***

*Institute of Materials Science, University of Silesia, Bankowa 12, 40-007 Katowice, Poland*

\*Corresponding author: [jozef.deniszczuk@us.edu.pl](mailto:jozef.deniszczuk@us.edu.pl)

### **Abstract**

The  $T$ - $x$  phase diagram of  $Zn_{1-x}Be_xSe$  alloy is calculated by means of *ab initio* method supplemented with the lattice Ising-like model cluster expansion approach and the Monte Carlo thermodynamic computations. Presented results confirm the high quality of mapping of disordered alloy onto the lattice Hamiltonian. The calculated phase diagram shows the asymmetric miscibility gap with the upper critical solution temperature equal to 860 K (1020 K) when the lattice vibrations are included (excluded) in the free energy of the system. We have proved that below the room temperature the miscibility of ZnSe and BeSe phases is possible only in the narrow range of concentration near the  $x = 0$  and 1. At elevated temperatures the two phases are more capable to be mixed over the wider concentration range on the Zn-rich side of phase diagram.

**Key words:** clamping, groove rolling, FEM

### **1. INTRODUCTION**

The alloying of semiconductors with the aim of tuning the band gap energy to achieve the values expected for device's application in recent past was the subject of extensive experimental and theoretical research (Berghout et al., 2007; and references cited therein). The investigations were focused especially on the wide-band gap II-IV semiconductors. The II-IV ZnSe compound is one of the promising materials for light emitting devices operating at short wavelengths (green and blue range). However the dislocations, point defects and their diffusion causes the degradation observed in the devices based on the ZnSe structures. Knowing that the BeSe compound is characterized by a strong covalent bonding (Vérité, 1997), the alloying of ZnSe with BeSe was proposed to increase the resistance of the ZnSe structure to defect generation (Plazaola et al., 2003).

Recent measurements have confirmed that the concentration of vacancies in  $Zn_{1-x}Be_xSe$  alloy decreases with increasing concentration of Be atoms (Plazaola et al., 2003). However, Raman scattering study of lattice dynamics in  $Zn_{1-x}Be_xSe$  alloy has proved that the atomic distribution in the alloy is not uniform but the ZnSe rich and BeSe rich regions form (Pagès et al., 2010). This findings indicate that the phase separation occurs in the samples investigated, what may indicate the presence of the immiscibility region in the ( $T$ - $x$ ) phase diagram of the alloy. Due to mismatch of unit cell volumes and different elastic properties of ZnSe and BeSe constituents the preparation of the  $Zn_{1-x}Be_xSe$  alloy may demand special conditions. The knowledge of the  $T$ - $x$  phase diagram might be very helpful in preparation of  $Zn_{1-x}Be_xSe$  alloy. The phase diagram of the  $Zn_{1-x}Be_xSe$  alloy was the subject of theoretical *ab initio* study with the use of the common tangent

method of phase diagram construction (Berghout et al., 2007). In the approach only formation enthalpy was taken into account, neglecting the lattice vibration contribution to the free energy of the system. Furthermore, in the phase diagram calculations the formation enthalpy for only few concentrations was considered.

The present work aims to extend the study phase stability of  $Zn_{1-x}Be_xSe$  system to cover both the configuration formation enthalpy and lattice vibrations free energy contributions to the total free energy of the system. With this aim the theoretical research was undertaken aimed to determine the  $T$ - $x$  phase diagram of  $Zn_{1-x}Be_xSe$  alloy by *ab-initio* method supplemented with the Monte Carlo (MC) phase diagram calculations within the semi-grand-canonical ensemble.

In the subsequent text the computational details are presented in Sec. 2. The results are presented and discussed in Sec. 3. Section 4 is the conclusion.

## 2. COMPUTATIONAL DETAILS

In the normal conditions the both end-member compounds, ZnSe and BeSe, crystallize in the zinc-blend (B3) type structure (Karzel et al., 1996; Luo et al., 1995). With this in mind, in our phase diagram calculations we assume the B3-type structure for  $Zn_{1-x}Be_xSe$  alloy for the entire concentration range. Formation energies,

$$\Delta E = E_{Zn_{1-x}Be_xSe} - xE_{BeSe} - (1-x)E_{ZnSe},$$

were calculated up to 20 atoms per unit cell. Total energy calculations were done using the Vienna *ab initio* Simulation Package VASP (Kresse & Hafner, 1993, 1994; Kresse & Furthmüller, 1996a, 1996b) using ultrasoft Vanderbilt-type pseudopotentials (Vanderbilt, 1990) with the generalized gradient approximation (GGA) for exchange and correlation. Valence electron configurations for the pseudopotentials are Se = 4s<sup>2</sup>4p<sup>4</sup>, Be = 2s<sup>2</sup>, Zn = 3d<sup>10</sup>4s<sup>2</sup>. All calculations were converged with respect to gamma centered k-point sampling, and a plane-wave energy cutoff of 350 eV was used which yields  $\Delta E$  values that are converged to within a few meV per atom. Electronic degrees of freedom were optimized with a conjugate gradient algorithm, which is recommended for difficult relaxation problems. Each superstructure was relaxed with respect to volume, supercell shape and atomic positions.

Based on the VASP results all remaining steps of the First Principles Phase Diagram (FPPD) calculations were performed with the use of Alloy Theo-

retic Automated Toolkit (ATAT) software package (van de Walle & Ceder, 2002a; van de Walle et al., 2002; van de Walle & Asta, 2002). In the first step VASP calculations were used to construct cluster expansion (CE) Hamiltonian. The cluster expansion (Sanchez et al., 1984) is a method to parameterize the energy of a material as a function of its configuration. The energy, (per atom) is represented as a polynomial in the occupation variables given by equation (1):

$$E(\sigma) = \sum_{\alpha} m_{\alpha} J_{\alpha} \left\langle \prod_{i \in \alpha} \sigma_i \right\rangle, \quad (1)$$

where  $\alpha$  is a cluster defined as a set of lattice sites. The sum is taken over all clusters  $\alpha$  that are not equivalent by a symmetry operation of the space group of the parent lattice, while the average is taken over all clusters  $\alpha'$  that are equivalent to  $\alpha$  by symmetry. The coefficients  $J_{\alpha}$  of CE expansion (1) embody the information regarding the energetics of the alloy and are called the Effective Cluster Interaction (ECI). The multiplicities  $m_{\alpha}$  indicate the number of clusters that are equivalent by symmetry to a divided by the number of lattice sites. Typical well-converged cluster expansion system contains of about 10-20 effective cluster interactions and requires the calculation of the energy of around 30-50 ordered structures (van de Walle et al., 2002; van der Ven et al., 1998; Garbulsky & Ceder, 1995; Ozolinš et al., 1998).

The predictive power of cluster expansion, defined by equation (1) is controlled by cross-validation score defined by equation (2)

$$CV = \left( \frac{1}{n} \sum_{i=1}^n (E_i - \hat{E}_{(i)})^2 \right)^{\frac{1}{2}} \quad (2)$$

where  $E_i$  is an *ab initio* calculated energy of superstructure  $i$ , while  $\hat{E}_{(i)}$  represent the energy of superstructure  $i$  obtained from CE (equation (1)) using the  $(n-1)$  other structural energies.

The part of the free energy contributed by lattice vibrations was taken into account employing the coarse-graining formalism. For each superstructure the vibrational free energy was calculated within the quasi-harmonic approximation. To reduce the computational time needed for obtaining phonon densities of states for a set of superstructures involved in the cluster expansion procedure, the bond-length-dependent transferable force constant approximation was used. Within the approximation the nearest-



neighbor force constant matrix as function of bond lengths (volume) was calculated for the end-members SeZn and SeBe of  $Zn_{1-x}Be_xSe$  series. For all remaining superstructures the force constant matrices were predicted using the relaxed bond lengths and the chemical identities of bonds in each superstructure and employing the bond stiffness versus bond length functions evaluated for end-member compounds. In this procedure, called transferable force constant approach (van de Walle & Ceder, 2002b), the force constant matrix is approximated by the diagonal form described by equation (3) (Liu et al., 2007)

$$\Phi_{i,j} = \begin{pmatrix} b & & \\ & b & \\ & & s \end{pmatrix}, \quad (3)$$

with only two independent terms: stretching stiffness  $s$ , and the isotropic bending stiffness  $b$ .

An alternative way to determine the vibrational free energy for each superstructure considered in the cluster expansion (1) is to apply the direct force method (Parlinski et al., 1997) or the linear response theory (Giannozzi et al., 1991), individually for each superstructure. Because of multiautomatic composition and low crystal symmetry of superstructures both alternative approaches demand high computing power and are time consuming, and are not applicable in the phase diagram calculations.

**Table 1.** Cluster coordinates and corresponding effective cluster interactions of clusters taken into account in cluster expansion series defined by equation (1).

Index	Cluster coordinates	$d_{i,j}^{(a)}$ , Å	ECI, eV/cation	Index	Cluster coordinates	$d_{i,j}^{(a)}$ , Å	ECI, eV/cation
1	Zero cluster		0.041703	8	(1,1,1) (0, 0, 2)	6.944	-0.001199
2	Point cluster		0.012845	9	(1,1,1) (-1/2, 0, 3/2)	7.501	-0.000661
3	(1, 1, 1) (1/2, 1, 3/2)	2.835	0.006974	10	(1,1,1) (-1, 1, 1)	8.019	-0.001201
4	(1,1,1) (0, 1, 1)	4.009	-0.003786	11	(1,1,1) (-1, 1/2, 3/2)	8.505	-0.001169
5	(1,1,1) (0, 1/2, 3/2)	4.910	-0.002446	12	(1,1,1) (-1/2, -1/2, 1)	8.505	0.000852
6	(1,1,1) (0, 0, 1)	5.670	0.003586	13	(1,1,1) (-1, 0, 1)	8.965	-0.000586
7	(1,1,1) (-1/2, 1/2, 1)	6.339	-0.001999	14	(1,1,1) (1/2, 1, 3/2) (1/2, 1/2, 1)	2.835	-0.002262

<sup>(a)</sup>  $d_{i,j}$  is the distance of the longest pair within the cluster

The phase diagram calculations were performed with the use of the Monte Carlo (MC) thermodynamic integration within the semi-grand-ensemble (van de Walle & Asta, 2002). The Hamiltonian used in MC integration was of the cluster expansion form given by equation (1) with expansion parameters fitted to the formation enthalpy and vibrational free energy calculated by parallel computing.

### 3. RESULTS AND DISCUSSION

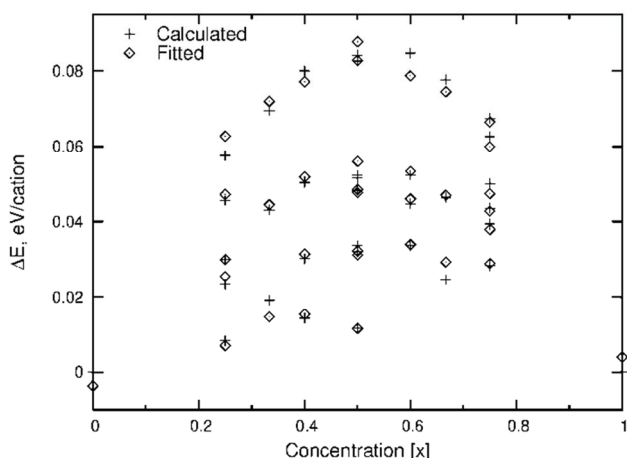
The *ab initio* calculations were performed for the end-member compounds ZnSe and BeSe and 33 reference superstructures containing up to 20 atoms. All supercell energies are positive with respect to end-member compounds, no intermediate ground states was found, what indicates a miscibility gap system. In the fitting procedure described in Sec. 2 the best cross-validation score ( $CV = 0.0051$ ) was obtained for 14 clusters in the expansion (1). The cluster coordinates and corresponding effective cluster interactions are collected in table 1. It is evident, that the largest ECI introduce the zero and point clusters. Among multisite clusters the largest ECI belongs to nearest neighbor cation sites. With increasing distance between sites of cluster the values of pair ECI falls down in an oscillatory manner.

Figure 1 shows the formation energies  $\Delta E$  (per cation atom) calculated for all reference superstructures by *ab initio* (VASP) method and using the cluster expansion (1) using the ECI given in table 1. The calculated and fitted energies do not coincide precisely, but besides the end-member compounds the residuals are at least one order of magnitude smaller than the values of  $\Delta E$  itself. This result confirms the quality of computational methodology and correct predictive power of CE expansion.

The bending and stretching bond stiffness versus bond length relationships for Se-Zn and Se-Be nearest neighbor bonds are presented in figure 2. The bond stiffness ( $b$  and  $s$ ) constants calculated base on the force constants determined *ab initio* within the small displacement approach the for



a sequence of volumes of end-member compounds show the linear dependence on bond length.



**Fig. 1.** Formation energies  $\Delta E$  calculated by VASP (cross) and fitted by cluster expansion

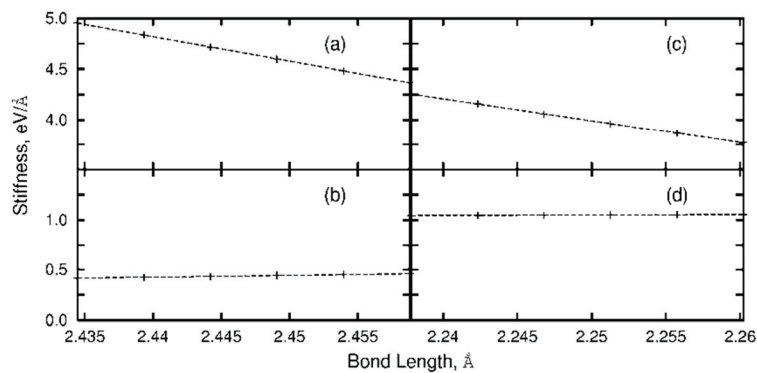


**Fig. 2.** Nearest neighbor stretching  $s$  (figures a, c) and bending  $b$  (figures b, d) force constants versus bond length for Se-Zn (left panel) and Be-Se (right panel) bonds. Crosses indicate an *ab initio* data points and lines represent linear fits used in the calculations of the vibrational free energy.

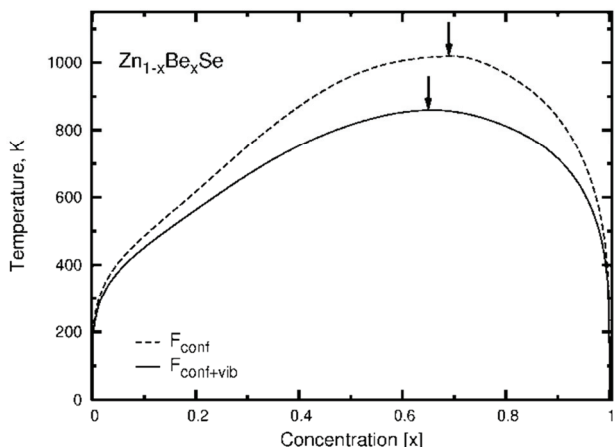


**Fig. 3.** Calculated phase diagram based on the ECI fitted to the configuration formation enthalpy (dash line) and on the temperature-dependent ECI fitted to the sum of configuration and vibration free energy (solid line). The arrows show the upper critical solution points.

Figure 3 shows the phase diagram of  $Zn_{1-x}Be_xSe$  alloy calculated on the base of temperature independent ECI (fitted to formation enthalpies) and temperature dependent ECI (fitted to the sum of formation enthalpies and vibration free energies).

The main feature of the calculated phase diagram is the presence of asymmetric miscibility gap with upper critical solution temperature ( $T_C$ ). With only the configurational degrees of freedom taken into account our modeling yields the critical point  $(x_c, T_C) = (0.69, 1020 \text{ K})$ . The shape of our phase diagram differs noticeably from that calculated by Berghout et al. (2007), where no asymmetry can be observed. The critical temperature obtained within the restricted (to formation enthalpies) approach ( $T_C = 1020 \text{ K}$ ) is significantly lower than the one obtained by Berghout et al. (2007) ( $T_C = 1324 \text{ K}$ ). Also the critical concentration ( $x_c = 0.54$ ) found by

Berghout et al. (2007) is much lower than our result. The higher critical concentration resulted from our calculations can be attributed to an asymmetry of the phase diagram (figure 3).

The contribution to free energy of vibrational degrees of freedom, when taken into account, modifies considerably the phase diagram (figure 3). The main effect of lattice vibrations is the shift of critical point to lower temperature ( $T_C = 860 \text{ K}$ ). The critical concentration remains almost unchanged ( $x_c = 0.65$ ). An effect of vibrations on the shape of phase diagram is negligible although the recess visible on the phase diagram resulted from formation enthalpies solely is reduced slightly.

The asymmetric shape of calculated phase diagram might suggest the presence on the Zn-rich left-hand side of concentration range of some additional structure with the ground-state configuration energy lower than that of end-member compounds. However our detailed search for the structures with negative ground-state formation enthalpy failed.

The asymmetry of the phase diagram, indicating the enhanced miscibility of cation atoms on the Zn-rich side of phase diagram, can be related to the mismatch of ionic radii of cation ions (Zn – 74 pm and Be – 41 pm). It is well known, that the miscibility gap between end-member compounds with ions with very different ionic radius are asymmetric with reduced solubility on the side of the diagram corresponding to the smaller ion (Burton et al., 2006).



## CONCLUSIONS

*Ab initio* based Monte Carlo modeling of  $x$ - $T$  phase diagram of  $Zn_{1-x}Be_xSe$  alloy has shown that in the normal condition the solubility of Zn and Be cations is possible only on the Zn-rich side of phase diagram. At elevated temperatures the two phases, ZnSe and BeSe, are more capable to be mixed over the wider concentration range on the Zn-rich side of phase diagram. The upper critical solution temperature of 860 K is predicted at concentration  $x = 0.65$  of Be, above which the solubility of cations is possible over the all concentration range.

## REFERENCES

- Berghout, A., Zaoui, A., Hugel, J., Ferhat, M., 2007, First-principles study of the energy-gap composition dependence of  $Zn_{1-x}Be_xSe$  ternary alloys, *Phys. Rev. B*, 75, 205112-205121.
- Burton, B.P., van de Walle, A., Kattner, U., 2006, First principles phase diagram calculations for the wurtzite-structure systems AlN-GaN, GaN-InN, and AlN-InN, *Journ. Appl. Phys.*, 100, 113528-113534.
- Garbulsky, G.D., Ceder, G., 1995, Linear-programming method for obtaining effective cluster interactions in alloys from total-energy calculations: Application to the fcc Pd-V system, *Phys. Rev. B*, 51, 67-72.
- Giannozzi, P., de Gironcoli, S., Pavone, P., Baroni, S., 1991, *Ab initio* calculation of phonon dispersions in semiconductors, *Phys. Rev. B*, 43, 7231-7242.
- Karzel, H., Potzel, W., Köfferlein, M., Schiessl, W., Steiner, M., Hiller, U., Kalvius, G.M., Mitchell, D.W., Das, T.P., Blaha, P., Schwarz, K., Pasternak, M.P., 1996, Lattice dynamics and hyperfine interactions in ZnO and ZnSe at high external pressures, *Phys. Rev. B*, 53, 11425-11438.
- Kresse, G., Hafner, J., 1993, *Ab initio* molecular dynamics for liquid metals, *Phys. Rev. B* 47, 558-561.
- Kresse, G., Hafner, J., 1994, *Ab initio* molecular simulation of the liquid-metal-amorphous-semiconductor transition in germanium, *Phys. Rev. B*, 49, 14251-14269.
- Kresse, G., Furthmüller, J., 1996a, Efficiency of *ab-initio* total energy calculations for metals and semiconductors using a plane-wave basis set, *Comput. Mater. Sci.*, 6, 15-50.
- Kresse, G., Furthmüller, J., 1996b, Efficient iterative schemes for *ab initio* total-energy calculations using a plane-wave basis set, *Phys. Rev. B*, 54, 11169-11186.
- Liu, J.Z., Gosh, G., van de Walle, A., Asta, M., 2007, Transferable force-constant modeling of vibrational thermodynamic properties in fcc-based Al-TM (TM = Ti, Zr, Hf) alloys, *Phys. Rev. B*, 75, 104117-15.
- Luo, H., Ghandehari, K., Greene, R.G., Ruoff, A.L., Trail, S.S., DiSalvo, F.J., 1995, Phase transformation of BeSe and BeTe to the NiAs structure at high pressure, *Phys. Rev. B*, 52, 7058-7064.
- Ozolinš, V., Wolverton, C., Zunger, A., 1998, Cu-Au, Ag-Au, Cu-Ag and Ni-Au intermetallics: First-principles study of temperature-composition phase diagram and structures, *Phys. Rev. B*, 57, 6427-64443.
- Pagès, O., Postnikov, A.V., Chafi, A., Bormann, D., Simon, P., Glas, F., Firszt, F., Paszkowicz, W., Tournie, E., 2010, Non-random Be-to-Zn substitution in ZnBeSe alloys: Raman scattering and *ab initio* calculations, *Eur. Phys. J. B*, 73, 461-469.
- Parlinski, K., Li Z.Q., Kawazoe, Y., 1997, First-principle determination of the soft mode in cubic  $ZrO_2$ , *Phys. Rev. Lett.*, 78, 4063-4066
- Plazaola, F., Flyktman, J., Saarinen, K., Dobrzynski, L., Firszt, F., Legowski, S., Meczynska, H., Paszkowicz, W., Reniewicz, H., 2003, Defect characterization of ZnBeSe solid solutions by means of positron annihilation and photoluminescence techniques, *J. Appl. Phys.*, 94, 1647-1653.
- Sanchez, J.M., Ducastelle, F., Gratias, D., 1984, Generalized cluster description of multicomponent systems, *Physica A*, 128, 334-350.
- Vanderbilt, D., 1990, Soft-selfconsistent pseudopotentials in a generalized eigenvalue formalism, *Phys. Rev. B*, 41, 7892-7895.
- van der Ven, A., Aydinol, M.K., Ceder, G., Kresse, G., Hafner, J., 1998, First-principles investigation of phase stability in  $Li_xCoO_2$ , *Phys. Rev. B*, 58, 2975-2987.
- van de Walle, A., Ceder, G., 2002a, Automating first-principles phase diagram calculations, *J. Phase Equilib.*, 23, 348-359.
- van de Walle, A., Asta, M., Ceder, G., 2002, The alloy theoretic automated toolkit: A user guide, *Calphad*, 26, 539-553.
- van de Walle, A., Asta, M., 2002, Self-driven lattice-model Monte Carlo simulations of alloy thermodynamic, *Modelling Simul. Mater. Sci. Eng.*, 10, 521-538.
- van de Walle, A., Ceder, G., 2002b, The effect of lattice vibrations on substitutional alloy thermodynamics, *Rev. Mod. Phys.*, 74, 11-45.
- Vérité, C., 1997, Expected pronounced strengthening of II-VI lattices with beryllium chalcogenides, *Mater. Sci. Eng. B*, 43, 60-64.

## OBLICZENIA Z PIERWSZYCH ZASAD DIAGRAMU FAZOWEGO UKŁADU ZnSe-BESE METODĄ CAŁKOWANIA TERMODYNAMICZNEGO MONTE CARLO

### Streszczenie

W pracy przedstawiono rezultaty badań teoretycznych stabilności fazowej roztworu stałego  $Zn_{1-x}Be_xSe$  w zależności od temperatury i koncentracji składników. Diagram fazowy  $T$ - $x$  wyznaczono na podstawie potencjału termodynamicznego wyliczonego metodą całkowania termodynamicznego Monte Carlo w ramach wielkiego rozkładu kanonicznego. W obliczeniach termodynamicznych wykorzystano Hamiltonian sieciowy w postaci tzw. rozwinięcia klastrowego (typu modelu Isinga). Współczynniki energetyczne rozwinięcia klastrowego wyznaczono drogą dopasowania Hamiltonianu sieciowego do wartości entalpii tworzenia wyliczonych kwantowymi metodami z pierwszych zasad dla 33 nadstruktur  $Zn_{1-x}Be_xSe$  w całym zakresie koncentracji. W obliczeniach termodynamicznych uwzględniono również wkład do energii swobodnej pochodzący od drgania sieci, który wyznaczono dla 33 nadstruktur w ramach przybliżenia kwazi-harmonicznego.

Uzyskany z obliczeń diagram fazowy  $T$ - $x$  charakteryzuje się asymetryczną luką mieszalności. Obliczenia termodynamiczne oparte wyłącznie na części konfiguracyjnej energii swobodnej



dają diagram fazowy z górnym punktem krytycznym:  $x_C = 0,69$  i  $T_C = 1020$  K. Uwzględnienie drgań sieci daje obniżoną temperaturę krytyczną  $T_C = 860$  K ( $x_C = 0,65$ ). Prezentowane badania wykazały, że poniżej temperatury pokojowej mieszalność faz ZnSe i BeSe jest możliwa wyłącznie w wąskich zakresach koncentracji ( $x \approx 0$  oraz  $x \approx 1$ ). W podwyższonej temperaturze,  $400\text{ K} < T < T_C$ , mieszalność faz ZnSe i BeSe jest możliwa również w roztworach  $\text{Zn}_{1-x}\text{Be}_x\text{Se}$  o wzbogaconej zawartości cynku.

*Received: September 20, 2012*

*Received in a revised form: November 19, 2012*

*Accepted: November 30, 2012*

